

OPTICAL PROPERTIES OF DENTAL BIOCERAMICS EVALUATED BY KUBELKA-MUNK MODEL

Humberto Naoyuki Yoshimura
Universidade Federal do ABC
Rua Santa Adélia, 166, 09210-580
Santo André, São Paulo, Brazil

Marcelo Mendes Pinto
Universidade Nove de Julho
Av. Dr. Adolpho Pinto, 109, 01156-050
São Paulo, São Paulo, Brazil

Erick de Lima and Paulo Francisco Cesar
Universidade de São Paulo
Av. Prof. Lineu Prestes, 2227, 05508-900
São Paulo, São Paulo, Brazil

ABSTRACT

Bioceramic prostheses have been widely used in restorative dentistry due to their superior aesthetics. The mechanical properties of bioceramics for dental prosthesis have been studied extensively. However, data regarding their optical properties are scarce, despite the fact that they are necessary for modeling and predicting the light interaction with restorations. The aim of this work was to investigate the optical behavior of bioceramics used for dental restorations by Kubelka-Munk (K-M) model. Samples of a vacuum-sintered porcelain and three ceramic composites (Al_2O_3 , $\text{Al}_2\text{O}_3\text{-ZrO}_2$, MgAl_2O_4) infiltrated with glass were prepared. Reflectance was measured using a spectrophotometer using white and black backgrounds. Scattering (S) and absorption (K) coefficients, determined by K-M model, varied significantly among the investigated materials. In all bioceramics, the value of absorption coefficient decreased strongly with the increase in wavelength, while the value of scattering coefficient increased or remained almost constant. In general, the value of scattering coefficient increased with the decrease in the material's transparency, but this tendency was not observed for the value of absorption coefficient. The optical properties were correlated with the material's microstructure and mean free path for light propagation. The results indicated that the scattering was the dominant mechanism that determined the light transmission in the investigated materials, but, in low wavelength range, the absorption also had a significant effect.

INTRODUCTION

The increasing demand for aesthetic materials in dentistry has pushed the development of novel all-ceramic systems. Besides excellent aesthetics, these materials have the advantage of relatively good strength, color stability, wear and abrasion resistance and biocompatibility.^{1,2} Nowadays, many all-ceramic systems are available for the construction of monolithic (inlays, onlays, overlays and crowns) or bilayered (crowns and fixed partial dentures – FPDs) restorations.³

Porcelains are aesthetic materials largely used in dentistry to construct varied types of restorations and prostheses.⁴⁻⁶ An all-ceramic dental restoration system for construction of 3-unit FPDs is based on the infiltration of glass into porous skeletons of ceramic crystal particles, which results in ceramic-glass composite materials.^{7,8} In 1990, In-Ceram Alumina (Vita-Zahnfabrik, Germany) prepared by this method was introduced in the market.⁹ First, a green preform is

prepared by slip casting of Al_2O_3 particles and platelets, which is partially sintered to enhance the strength, but with minimum shrinkage to guarantee good marginal fit. Afterwards, the pre-sintered preform is covered with a lanthanum-aluminum silicate glass powder and then heat-treated to promote spontaneous infiltration.⁷⁻¹⁰ The microstructure of this composite has around 68 vol.% alumina, 27 vol.% glass, and 5 vol.% porosity.¹¹ The same manufacturer also developed two others composites, In-Ceram Spinel (with MgAl_2O_4 particles) and In-Ceram Zirconia (with Al_2O_3 and ZrO_2 particles).¹²

Bioceramic prostheses have been widely used in restorative dentistry due to their superior aesthetics. However, data regarding their optical properties are scarce, despite the fact that they are necessary for modeling and predicting light interaction within a restoration. Similarly to what happens to the dental tissues and other materials, a light beam is attenuated by passing through a solid ceramic, due to the interaction between light and matter by intrinsic absorption of the material and the scattering by optical heterogeneities. The main optical heterogeneities in ceramic materials are surfaces, secondary phases (including pores) and grain boundaries. The dispersion of the light beam occurs through the interfaces when there is a difference in the refractive index between the two phases; the higher the difference, the higher the scattering intensity. Light scattering by residual pores strongly affects the light transmission, because of the significant difference between the refractive index of ceramic and vacuum or entrapped gas. Mie scattering model explains the pore size dependence and predicts that maximum scattering occurs when the pores are almost as large as the wavelength of the incident light. Scattering and absorption from second-phase particles, also affect light transmission.^{13,14}

Most studies in bioceramics for dental restorations compared the material translucency on a relative scale named contrast ratio.^{15,16} From this measurement, however, the intrinsic properties of materials cannot be obtained. The Kubelka-Munk (K-M) model has been widely used to describe and predict the optical behavior of a turbid media, like intensely light-scattering, translucent materials.¹⁷ In this method, the reflectance is measured using white and black backgrounds for the determination of absorption (K) and scattering (S) coefficients.¹⁸

The aim of this work was to investigate the optical behavior of bioceramics used for dental restorations by Kubelka-Munk (K-M) model.

EXPERIMENTAL

A commercial dental porcelain powder was used: Veneer Material 7 - VM7 (Vita Zahnfabrik, Germany), which is a vitreous porcelain indicated as veneering material for glass-infiltrated alumina cores and can also be used in all-ceramic restorations. The green specimens (14.9 mm in diameter and 2.9 mm in thickness) were prepared by the vibration-condensation method and vacuum sintered in a dental porcelain furnace (Kerammat I, Knebel, Brazil) following the firing schedules recommended by the manufacturers (910°C maximum temperature).

The InCeram composites (Vita Zahnfabrik, Germany) were processed by infiltrating a lanthanum-silicate glass into a porous partially sintered ceramic preform (Al_2O_3 - InCeram Alumina, Al_2O_3 - ZrO_2 - InCeram Zirconia, MgAl_2O_4 - InCeram Spinel). Green bodies were prepared by slip casting the ceramic particle slurry into a mold consisted of a gypsum substrate and lateral walls of silicone. The casting direction was perpendicular to the largest surface of the disc. Green bodies were slightly sintered between 1120 and 1180°C for 2 to 3 h in air to prepare preforms with sufficient strength to handle. A low sintering temperature was used to avoid undesirable shrinkage of ceramic preforms. After applying the glass powder over the preform, glass was spontaneously infiltrated at 1110°C for 30 min (InCeram Alumina) and 1140°C for 50 min (InCeram Zirconia and Spinel). Both heating cycles, sintering and infiltration, were carried out in a specific furnace (InCerammat II, Vita Zahnfabrik, Germany).

In order to minimize the possible effects caused by the difference of color among the materials, the evaluated bioceramics in this study presented predominantly A2 color in the Vita color scale (Vita Zahnfabrik, Germany).

All samples were machined following the guidelines in ASTM C 1161 and the flat surfaces of each disc were mirror polished using a polishing machine (Ecomet 3, Buehler, USA) with diamond suspensions (45, 15, 6 and 1 μm). The final dimensions of the samples were: $\text{Ø}12 \times 0.5 \text{ mm}$. Ten discs were prepared for each bioceramic.

Reflectance was measured in a spectrophotometer (U-3000/3300, Hitachi, Japan), attached with an integrating sphere (ϕ 150 mm), at a step of 1 nm and scan rate of 300 nm/min, using white and black backgrounds (AG-5330, BYK Gardner, USA) with a thin film of glycerol between the disk and the background to avoid unwanted scattering from back surface of the specimen. The scattering (S) and absorption (K) coefficients were determined by Kubelka-Munk (K-M) model using the following equations:^{18,19}

$$R_{\text{med}} = r_1 + \frac{(1-r_1)(1-r_2)R^*}{1-r_2R^*} \quad (1)$$

$$r_1 = \frac{(n-1)^2}{(n+1)^2} \quad (2)$$

$$r_2 = 1 - \frac{1-r_d}{n^2} \quad (3)$$

$$r_d = \frac{1}{2} + \frac{(n-1)(3n+1)}{6(n+1)^2} + \frac{n^2(n^2-1)^2}{(n^2+1)} \ln\left(\frac{n-1}{n+1}\right) - \frac{2n^3(n^2+2n-1)}{(n^2+1)(n^4-1)} + \frac{8n^4(n^4+1)}{(n^2+1)(n^4-1)^2} \ln(n) \quad (4)$$

$$a = \frac{1}{2} \frac{R_{\text{sw}}^* R_w R_b - R_{\text{sw}}^* R_w R_{\text{sb}}^* + R_b - R_{\text{sb}}^* - R_w R_{\text{sb}}^* R_b - R_w + R_{\text{sw}}^* R_{\text{sb}}^* R_b + R_{\text{sw}}^*}{R_b R_{\text{sw}}^* - R_w R_{\text{sb}}^*} \quad (5)$$

$$b = \sqrt{a^2 - 1} \quad (6)$$

$$S = \frac{1}{bX} \coth^{-1} \left(\frac{aR_w^* + aR_{\text{sw}}^* - R_{\text{sw}}^* R_w^* - 1}{bR_w^* - bR_{\text{sw}}^*} \right) \quad (7)$$

$$K = S(a - 1) \quad (8)$$

where, n is the refraction index of the material, R is reflectance and subscript med, w, b, sw and sb are white background, black background, specimen with white background and specimen with black background, respectively.

A microstructural analysis of the bioceramics was performed using a scanning electron microscope, SEM (Quanta 600 FEG, FEI Holland). Volume fractions of second-phases were evaluated using an image analyzer (QWin, Leica, Germany) and five SEM micrographs of the polished transverse section of each material. These micrographs were also used for the measurement of mean free path for light propagation using the mean linear intercept method

(ASTM E 112). The mean free path is the average distance travelled by light inside the bioceramic without the occurrence of scattering at the interfaces between the different phases. In this method, ten lines were drawn on each micrograph in the same direction of the light propagation. In these lines, each phase change or presence of pore was considered as an intercept. The mean free path was then calculated dividing the total length of the line by the total number of intercepts. The volume fraction of pores was determined using the image analyzer and ten optical micrographs (DMRXE, Leica, Germany) of polished sections of each material.

RESULTS AND DISCUSSION

Figure 1 shows SEM micrographs of the prepared bioceramics. All materials presented residual pores. Table I shows the volume fractions of pores and crystals and the mean free path of bioceramics. The microstructure of porcelain VM7 had a homogeneous glassy matrix and after etching with HF solution the previous powder boundaries could be observed (Fig. 1a). The composite InCeram Alumina had elongated Al₂O₃ particles (74.7%v) dispersed in the glassy matrix (Fig. 1b). The composite InCeram Spinel had equiaxed MgAl₂O₄ particles (73.7%v) dispersed in the glassy matrix (Fig. 1c). The composite InCeram Zirconia presented particles of Al₂O₃ (61.8%v) and ZrO₂ (20.1%v, particles with light color in Fig. 1d) dispersed in the glassy matrix. Among the composites, the mean free path was higher in the InCeram Spinel especially because of its relative large MgAl₂O₄ particles and InCeram Zirconia had the lower value because of its higher volume fraction of crystalline particles.

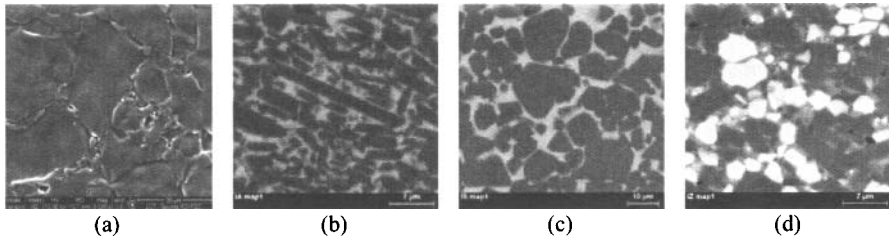


Figure 1. SEM images of the prepared bioceramics: (a) porcelain VM7; (b) InCeram Alumina; (c) InCeram Spinel; (d) InCeram Zirconia.

Table I. Volume fractions of pores and crystals and mean free path of bioceramics (values shown as mean ± standard deviation).

Bioceramic	%v pores	%v crystals	Mean free path (µm)
Porcelain	4.2 ± 1.6	0	---
InCeram Alumina	0.5 ± 0.2	74.7 ± 2.7	1.30 ± 0.14
InCeram Spinel	1.3 ± 0.7	73.7 ± 2.0	3.26 ± 0.88
InCeram Zirconia	1.6 ± 0.7	81.9 ± 6.5	1.22 ± 0.08

Figure 2 shows the results of reflectance measured with white and black backgrounds of the prepared bioceramics in the 300 to 800 nm wavelength range. The difference between the reflectance curves measured with white and black backgrounds is related with the translucency of the material. Therefore, the most translucent bioceramics were porcelain (Fig. 2a) and composite InCeram Spinel (Fig. 2c), followed by composite InCeram Alumina (Fig. 2b); the most opaque material was composite InCeram Zirconia (Fig. 2d). These results were in accordance with the visual (naked eyes) inspection. Note that the bioceramics were opaque or

had very low transparency in the ultraviolet region (300 to 400 nm), while higher transmissions were observed in the near-infrared region (above 700 nm).

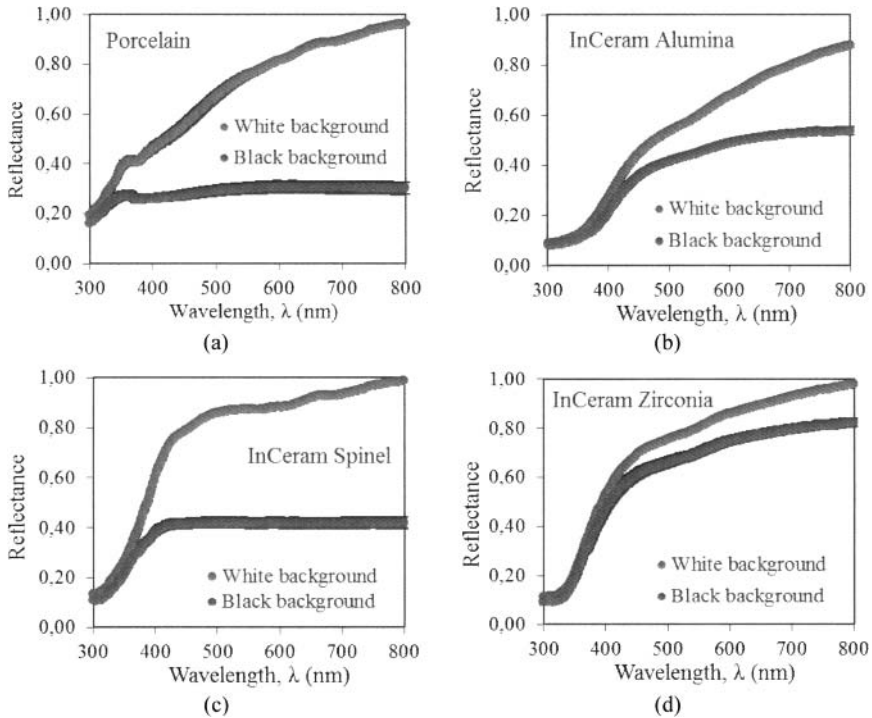


Figure 2. Results of reflectance (average of ten specimens) of: (a) porcelain VM7; (b) InCeram Alumina; (c) InCeram Spinel; (d) InCeram Zirconia. The standard-deviations are shown in black color (only those bigger than the size of the points are visible).

Usually pore is the main cause of the decrease in light transmission in a material due to its strong effect on light scattering and absorption.¹⁴ However, in this work, the differences in optical behavior observed among the evaluated bioceramics were not correlated with the porosity, since the most translucent bioceramic was the porcelain (Fig. 2a), which had the highest volume fraction of pores (4.2%v, Table I). Even among the composites, there was no correlation, since InCeram Alumina, which had the lowest porosity (0.5%v) was less translucent (Fig. 2b) than InCeram Spinel (Fig. 2c). A positive correlation was observed between translucency and mean free path parameter (Table I). The absence of crystalline phase and large $MgAl_2O_4$ particles in the porcelain and InCeram Spinel, respectively, caused less deviation of the light during its propagation (less scattering), resulting in higher light transmissions. On the other hand, the lower mean free paths in the composites InCeram Alumina and InCeram Zirconia caused more light scattering at the interfaces between crystalline particle and glassy matrix, which reduced significantly the light transmission. The mean free path is not the unique parameter determining the degree of light scattering at the crystal-glass interface in the

composites. The difference between the refractive indexes of these phases is also important. Therefore, matching this index in both phases minimizes light scattering. This is difficult to attain in multicrystalline composites, like in the InCeram Zirconia, since the refractive indexes of Al_2O_3 and ZrO_2 are very different (1.76 and 2.19, respectively)²⁰ and the refractive index of the glass cannot match simultaneously both crystalline phases, resulting in a bioceramic with low translucency.

Figure 3 shows the calculated scattering and absorption coefficients of Kubelka-Munk (K-M) model in the visible region (400 to 700 nm wavelength range), using the results of reflectance (Fig. 2).

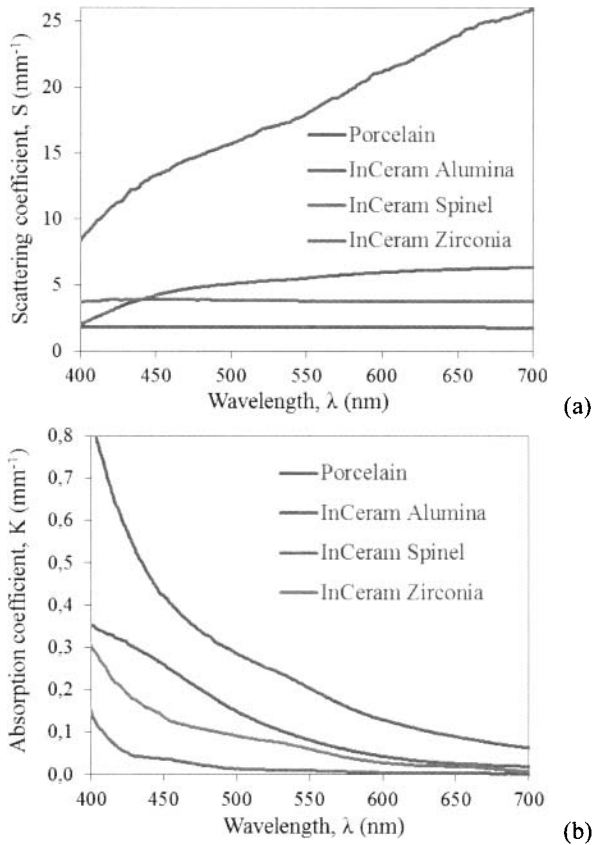


Figure 3. Coefficients of scattering, S (a), and absorption, K (b), of Kubelka-Munk model.

The scattering (S) and absorption (K) coefficients varied significantly among the investigated materials (S from 2 to 26 mm^{-1} and K from 0.85 to 0.002 mm^{-1} , between 400 and 700 nm). In all bioceramics, K value strongly decreased with the increase in wavelength (Fig. 3b), while S value increased (composites InCeram Alumina and InCeram Zirconia) or remained

almost constant (porcelain and composite InCeram Spinel) with the increase in wavelength (Fig. 3a). In general, the value of scattering coefficient was higher for material with lower transparency, but similar tendency was not observed for the value of absorption coefficient. The S value tended to increase with the decrease in mean free path for light propagation (Table I). The results indicated that the scattering was the dominant mechanism that determined the light transmission in the investigated materials, but, in low wavelength range, the absorption also affected significantly.

The scattering coefficient values of the porcelain and InCeram Spinel had small variations with the wavelength, but the values of the composites InCeram Alumina and InCeram Zirconia increased with the increase in the wavelength (Fig. 3a). The behavior of scattering coefficient of these composites seems to be related with the presence of high fractions of small submicron crystalline particles (Fig. 1), which interact strongly with the light in the range of visible wavelength (Mie scattering model).¹⁴ The increase in the absorption coefficient values with the decrease in the wavelength for all bioceramics (Fig. 3b) is related with the transmittance cut-off at the UV (ultraviolet) region and probably with the colorant additives used in these materials to achieve the A2 shade (color).

The values of S and K coefficients determined in this work for VM7 porcelain was similar to those reported for dental porcelains in the literature. Cook and McAree analyzed dental porcelains and composite resins by the Kubelka-Munk (K-M) model in the visible region.²¹ For two porcelains, they reported S values ranging from ~ 0.5 to $\sim 1.5 \text{ mm}^{-1}$ and K values from ~ 0.02 to $\sim 0.4 \text{ mm}^{-1}$,²¹ close to the values of S ($\sim 1.8 \text{ mm}^{-1}$, Fig. 3a) and K (0.008 to 0.34 mm^{-1} , Fig. 3b) determined in this work for VM7 porcelain. For two composite resins, the reported values varied from ~ 0.2 to $\sim 2 \text{ mm}^{-1}$ for S coefficient and ~ 0.04 to $\sim 1 \text{ mm}^{-1}$ for K coefficient.²¹ These values are close to the porcelains, because composite resins are usually highly translucent materials. For the ceramic composites analyzed in this work (InCeram systems), the K values were similar (ranged from 0.002 to 0.85 mm^{-1}), but the S values (ranged from 2.3 to 26 mm^{-1}) were significantly higher than those of the composite resins. Therefore, the coefficients of the K-M model of inorganic (ceramic) and organic (resin) commercial composites are not similar. It seems that there is no other study in the literature reporting the S and K values for InCeram composites.

CONCLUSIONS

The scattering (S) and absorption (K) coefficients, determined by Kubelka-Munk (K-M) model, varied significantly among the investigated materials (S from 2 to 26 mm^{-1} and K from 0.85 to 0.002 mm^{-1} , between 400 and 700 nm).

For all bioceramics, the value of K strongly decreased with the increase in wavelength. The value of S increased (Al_2O_3 - and $\text{Al}_2\text{O}_3\text{-ZrO}_2$ -composites) or remained almost constant (porcelain and MgAl_2O_4 -composite) with the increase of wavelength.

In general, the value of S increased with the lowering of transparency of the material, but similar tendency was not observed for the value of K.

The results indicated that the scattering was the dominant mechanism that determined the light transmission in the investigated materials, but, in low wavelength range, the absorption also affected significantly.

This work showed that the scattering coefficients of commercial ceramic composites (Al_2O_3 , $\text{Al}_2\text{O}_3\text{-ZrO}_2$, MgAl_2O_4) infiltrated with glass (InCeram systems) are significantly higher than the dental porcelains. In order to develop new more translucent glass-infiltrated ceramic composites it is necessary to decrease the scattering at the interfaces between the glass and ceramic phases.

ACKNOWLEDGMENTS

The authors acknowledge the Brazilian agencies FAPESP, CAPES and CNPq for the financial support of the present research.

REFERENCES

- ¹C.C. Gonzaga, P.F. Cesar, C.Y. Okada, C. Fredericci, F. Beneduce Neto, and H.N. Yoshimura, Mechanical Properties and Porosity of Dental Glass-Ceramics Heat-Pressed in Different Temperatures, *Mater. Res.*, **11**, 303-08 (2008).
- ²H.N. Yoshimura, C.C. Gonzaga, P.F. Cesar, and W.G. Miranda Jr., Relationship Between Elastic and Mechanical Properties of Dental Ceramics and Their Index of Brittleness, *Ceram. Int.*, **38**, 4715-22 (2012).
- ³M. Borba, M.D. de Araújo, E. de Lima, H.N. Yoshimura, P.F. Cesar, J.A. Griggs, and Á. Della Bona, Flexural Strength and Failure Modes of Layered Ceramic Structures, *Dent. Mater.*, **27**, 1259-66 (2011).
- ⁴R.M.C. Sasahara, F.C. Ribeiro, P.F. Cesar, and H.N. Yoshimura, Influence of the Finishing Technique on Surface Roughness of Dental Porcelains with Different Microstructures, *Oper. Dent.*, **31**, 577-83 (2006).
- ⁵H.N. Yoshimura, P.F. Cesar, F.N. Soki, and C.C. Gonzaga, Stress Intensity Factor Threshold in Dental Porcelains, *J. Mater. Sci. Mater. Med.*, **19**, 1945-51 (2008).
- ⁶C. Fredericci, H.N. Yoshimura, A.L. Molisani, M.M. Pinto, and P.F. Cesar, Effect of Temperature and Heating Rate on the Sintering of Leucite-Based Dental Porcelains, *Ceram. Int.*, **37**, 1073-78 (2011).
- ⁷C.C. Gonzaga, H.N. Yoshimura, P.F. Cesar, and W.G. Miranda Jr., Subcritical Crack Growth in Porcelains, Glass-Ceramics and Glass-Infiltrated Alumina Composite for Dental Restorations, *J. Mater. Sci. Mater. Med.*, **20**, 1017-24 (2009).
- ⁸C.C. Gonzaga, C.Y. Okada, P.F. Cesar, W.G. Miranda Jr., and H.N. Yoshimura, Effect of Processing Induced Particle Alignment on the Fracture Toughness and Fracture Behavior of Multiphase Dental Ceramics, *Dent. Mater.*, **25**, 1293-301 (2009).
- ⁹L. Probst and J. Diehl, Slip-Casting Alumina Ceramics for Crown and Bridge Restorations, *Quintessence Int.*, **23**, 25-31 (1992).
- ¹⁰S.O. Koutayas, All-Ceramic Posts and Cores: the State of the Art, *Quintessence Int.*, **30**, 383-92 (1999).
- ¹¹M. Guazzato, M. Albakry, S.P. Ringer, and M.V. Swain, Strength, Fracture Toughness and Microstructure of a Selection of All-Ceramic Materials. Part I. Pressable and Alumina Glass-Infiltrated Ceramics, *Dent. Mater.*, **20**, 441-48 (2004).
- ¹²M. Guazzato, M. Albakry, M.V. Swain, and J. Ironside, Mechanical Properties of In-Ceram Alumina and In-Ceram Zirconia, *Int. J. Prosthodont.*, **15**, 339-46 (2002).
- ¹³H.N. Yoshimura, A.C. Camargo, E.P. Goulart, and K. Maekawa, Translucent Polycrystalline Alumina: Influence of Roughness and Thickness on In-Line Transmittance, *Mater. Sci. Forum*, **299-300**, 35-43 (1999).
- ¹⁴H.N. Yoshimura and H. Goldenstein, Light Scattering in Polycrystalline Alumina with Bi-Dimensionally Large Surface Grains, *J. Eur. Ceram. Soc.*, **29**, 293-303 (2009).
- ¹⁵S.A. Antonson and K.J. Anusavice, Contrast Ratio of Veneering and Core Ceramics as a Function of Thickness, *Int. J. Prosthodont.*, **14**, 316-20 (2001).
- ¹⁶M.J. Heffernan, S.A. Aquilino, A.M. Diaz-Arnold, D.R. Haselton, C.M. Stanford, and M.A. Vargas, Relative Translucency of Six All-Ceramic Systems. Part II: Core and Veneer Materials, *J. Prosthet. Dent.*, **88**, 10-15 (2002).
- ¹⁷L. Yang and B. Kruse, Revised Kubelka-Munk Theory I. Theory and Application, *J. Opt. Soc. Am.*, **21**, 1933-41 (2004).

¹⁸J.C. Ragain and W.M. Johnston, Accuracy of Kubelka-Munk Reflectance Theory Applied to Human Dentin and Enamel, *J. Dent. Res.*, **80**, 449-52 (2001).

¹⁹M.B. Thomas and R.H. Doremus, Characterizing Opacity of Translucent Ceramic Materials, *J. Am. Ceram. Soc.*, **59**, 229-32 (1976).

²⁰M.W. Barsoum, *Fundamentals of Ceramics*, Bristol, IOP Publishing, 2003.

²¹W.D. Cook and D.C. McAree, Optical Properties of Esthetic Restorative Materials and Natural Dentition, *J. Biomed. Mater. Res.*, **19**, 469-88 (1985).